Peptide Inhibitors of HIV-1 Integrase Dissociate the Enzyme Oligomers†

Richard G. Maroun,‡,§ Stéphanie Gayet,‡ Mohamed S. Benleulmi,‡ Horea Porumb,‡ Loussinée Zargarian,‡ Hayate Merad,‡ Hervé Leh,|| Jean-François Mouscadet,|| Frédéric Troalen,⊥ and Serge Fermandjian*,‡

Département de Biologie et Pharmacologie Structurales, Laboratoire de Physicochimie et de Pharmacologie des Macromolécules Biologiques, and Laboratoire de Microchimie et d'Immunologie Moléculaire, Département de Biologie Clinique, UMR 8532 CNRS, Institut Gustave Roussy, 94805 Villejuif, France, and Département des Sciences de la Vie et de la Terre, Faculté des Sciences, Université Saint Joseph, CST-Mar Roukos, B.P. 1514, Beyrouth, Liban

Received June 25, 2001; Revised Manuscript Received August 30, 2001

ABSTRACT: Integration of HIV-1 genome into host cell chromosome is mediated by viral integrase (IN). The IN catalytic core (CC, IN^{50-212}) dimerizes through mutual interactions of its α1 and α5 helices. Peptides INH1 and INH5 reproducing these helix sequences strongly inhibited IN. For instance, an IC_{50} of 80 nM was determined for INH5 in integration assays using wild-type IN (wtIN). In size exclusion chromatography, INH1 and INH5 perturbed the association−dissociation equilibrium of both dmIN (IN^{1-288}/F185K/C280S) and CC, leading to monomers as surviving species, while in circular dichroism, binding of peptides to dmIN altered the protein conformation. Thus, enzyme deactivation, subunit dissociation, and protein unfolding are events which parallel one another. The target of INH5 in the enzyme was then identified. In fluorescence spectroscopy, $C_{0.5}$ values of 168 and 44 nM were determined for the binding affinity of INH5 to IN and CC, respectively, at 115 nM subunit concentration, while interaction of INH5 with INH1 was found stronger than interaction of INH5 with itself (23 times larger in term of dissociation constants). These results strongly suggested that the α1 helix is the privileged target of INH5. The latter could serve as a lead for the development of new chemotherapeutic agents against HIV-1.

The virus-encoded human immunodeficiency virus type 1 (HIV-1)[1] integrase (IN) is essential for the viral replication cycle (for a review, see refs *1*−*8*). It is thus an obvious candidate for antiviral chemotherapy besides the commonly used targets reverse transcriptase and protease. Yet, progress with the design of integrase inhibitors is still slow, a major difficulty being the absence of compounds displaying good specificity for IN (for a review, see refs *9*−*12*).

HIV-1 IN is a 32 kDa polynucleotidyltransferase that catalyzes the integration of the DNA copy of the viral genome in a two-step reaction, each proceeding by direct transesterification (*3*). The 3′ processing occurs in the cytoplasm and the DNA strand transfer in the nucleus of the infected cell. A wealth of experimental results suggests a three-domain structure for HIV-1 IN (*7*): the N-terminal domain (residues 1−51); the central domain CC (residues 52−210) containing the highly conserved catalytic acidic residues Asp-64, Asp-116, and Glu-152; and the C-terminal domain (residues 220−288) rich in basic residues. The whole protein is required for processing and DNA strand transfer reactions, while CC is able to carry out the disintegration reaction on its own (*13*).

The three-dimensional structure of each domain is now well-known (*5*, *14*−*20*). Each forms a dimer in solution, although the full enzyme is likely to function as at least a tetramer (*4*). Several crystal structures of the CC domain (residues 50−212) have been determined (*5*, *14*−*17*). More recently the first IN multidomain crystal structure has been reported, including the CC and the C-terminal domains (residues 52−288) (*21*). The protein assumes a Y-shaped dimer structure, where the CC domains are at the dimer interface and the C-terminal domains point away from each other. In all the structures so far reported, the dimer interface involves the strong helix-to-helix contacts α1:α5′ and α5:α1′, where both hydrophobic and electrostatic interactions contribute to dimer stabilization (Figure 1) (*15*).

Here, we report on the inhibitory properties and inhibition mechanism of 2 synthetic peptides: INH1 that reproduces the amino acid sequence of the α1 helix (17 residues from amino acids 93−107); and INH5 that incorporates the α5 helix and a part of the loop separating the α4 and α5 helices (21 residues from amino acids 167−187). INH1 and INH5 present mostly unordered structures in aqueous solution, but they gain in helicity upon addition of trifluoroethanol (TFE),

† This work was supported by SIDACTION and the Agence Nationale de la Recherche sur le SIDA, France. R.G.M. and L.Z. are holders of grants from SIDACTION.

* To whom correspondence should be addressed at the Département de Biologie et Pharmacologie Structurales, UMR 8532 CNRS, Institut Gustave Roussy, 39 rue Camille Desmoulins, 94805 Villejuif, France. Tel: +33 1 42 11 49 85. Fax: +33 1 42 11 52 76. E-mail: sfermand@igr.fr.

‡ Département de Biologie et Pharmacologie Structurales, Institut Gustave Roussy.

§ Département des Sciences de la Vie et de la Terre, Université Saint Joseph.

|| Laboratoire de Physicochimie et de Pharmacologie des Macromolécules Biologiques, Institut Gustave Roussy.

⊥ Laboratoire de Microchimie et d'Immunologie Moléculaire, Institut Gustave Roussy.

[1] Abbreviations: HIV, human immunodeficiency virus; IN, integrase; dmIN, double mutant integrase; wtIN, wild-type integrase; CC, catalytic core; SEC, size exclusion chromatography; CD, circular dichroism; TFE, 2,2,2-trifluoroethanol; CHAPS, 3-[(3-cholamidopropyl)dimethylammonio]-1-propanesulfonate; EDTA, ethylenediaminetetraacetic acid.

10.1021/bi011328n CCC: $20.00
Published on Web 10/26/2001

reflecting a propensity to mimic the structure of their homologous helical segments, α1 and α5 (*14*−*17*). INH5 was a better inhibitor of IN than INH1 in in vitro heterointegration (strand transfer) assays using dmIN$^{1-288}$/F185K/C280S at 280 nM and Mn^{2+} as a divalent cation (IC_{50} = 0.5 and 250 μM, respectively). INH5 manifested a still better inhibitory activity (IC_{50} about 85 nM) toward wtIN used at a 50 nM concentration in the presence of Mg^{2+}.

Many types of IN inhibitors including peptides have been identified so far (*9*, *22*). Referring to these results, INH5 appears as one of the best peptide inhibitors ever prepared against IN. In size exclusion chromatography (SEC), both INH5 and INH1 dissociated the associated species of dmIN and of CC into monomers. The dmIN monomers displayed a longer retention time compared to the unliganded monomers, suggesting a possible alteration of their conformation. Actually, circular dichroism (CD) analysis confirmed the change of the secondary structure of IN produced by the binding of INH1 and INH5 to the enzyme, paralleling therefore the disruption of the oligomer species shown by SEC. The consistency among the bioassay, SEC, and CD results strongly suggests that INH1 and INH5 prevent the formation of functional oligomers. Concerning the binding sites of these inhibitors, the higher stability of the INH1:INH5 heterocomplex compared with the homocomplexes INH5:INH5 and INH1:INH1 suggested that the α1 helix (α5 helix, respectively), normally interacting with the α5′ helix (α1′ helix, respectively) at the dimer interface, is the preferential target of INH5 (INH1, respectively) in the protein. Fluorescence data show that INH5 interacts much more strongly with the enzyme and its CC domain than with the INH1 peptide (at least by a factor of 100) and more strongly with INH1 than with itself (by a factor of 23), indicating that the targets of INH5 and INH1 are located in the CC domain and are presumably constituted by the α1 and α5 helices, respectively.

EXPERIMENTAL PROCEDURES

Peptides and Oligonucleotides. Peptides INH1 (AT-GQETAYFLLKLAGKA-$CONH_2$) and INH5 (DQAEHLK-TAVQMAVFIHNYKA-$CONH_2$) were derived from the IN sequence 93−107, by addition of Ala at both the N- and C-termini and replacement of Arg-107 with Lys and, respectively, from the sequence 167−187, by replacement of antepenultimate Phe with Tyr and C-terminal Arg with Ala. They were synthesized according to the Fmoc procedure on an Applied Biosystems model 432A automatic solid phase synthesizer and were purified by reverse-phase HPLC on an aquapore column using a linear gradient from 0 to 100% acetonitrile, 0.1% trifluoroacetic acid in water. The molecular mass of each peptide was determined by electrospray ionization mass spectrometry (ESIMS) on the Platform-quadrupole instrument (VG Biotech). Peptide concentrations were determined by UV absorption using the molar absorption coefficient at 280 nm equal to 1197 $M^{-1}\cdot cm^{-1}$. A fluorescent version of INH5 was obtained by direct incorporation, during automatic synthesis, of an N-terminal anthraniloyl-lysine residue. The anthraniloyl moiety is attached to the ϵ-amino group of Lys (*23*).

Oligonucleotides S1 (5′-GTGTGGAAAATCTCTAGCA), S2 (3′-CACACCTTTTAGAGATCGTCA), S3 (5′-GTGTGGAAAATCTCTAGCAGT), and DIN (dumbdell substrate) (5′-TGCTAGTTCTAGCAGGCCCTTGGGCCGGCGCTTGCGCC), used in the heterointegration assays in vitro with pSP65 DNA (strand transfer activity) (S1/S2) and in the autointegration assays (S2/S3), were prepared by the phosphoroamidite procedure in our laboratory.

Proteins. (A) Double Mutant IN (dmIN). This mutant was prepared because of its better solubility, to use it in size-exclusion chromatography and CD experiments, which require higher protein concentrations. Plasmid encoding dmIN (IN$^{1-288}$/F185K/C280S) was kindly provided by R. Craigie (NIH). The enzyme was expressed in *Escherichia coli* strain BL21(DE3) as previously described (*24*). Purification was performed at 4 °C under native conditions on Ni−NTA spin columns (Qiagen). Cells expressing dmIN from 250 mL of culture media were resuspended in 10 mL of lysis buffer (40 mM imidazole in Buffer A: 20 mM Hepes, pH 7.5, 1 M NaCl, 10 mM CHAPS). The cell suspension was incubated 30 min at 4 °C in the presence of 1 mg/mL lysozyme and sonicated. The lysed cells were centrifuged 30 min at 10000*g*, and the supernatant was filtered (0.22 μm) and loaded onto Ni−NTA columns (Qiagen) equilibrated with lysis buffer. The columns were washed with Buffer A plus 100−150 mM imidazole, and the protein was eluted with Buffer A plus 700 mM imidazole. The fractions containing IN were pooled and dialyzed overnight against storage buffer [20 mM Hepes, pH 7.5, 1 M NaCl, 1 mM DTT, 50 μM $ZnCl_2$, and 10% (w/v) glycerol]. The concentrations of purified dmIN were determined with the Bradford kit (Promega) and by UV absorption using a calculated extinction coefficient of 46 542 M^{-1} cm^{-1} at 280 nm, based on the amino acid composition. Finally, aliquots of purified enzyme were stored at −80 °C.

(B) Wild-Type IN (wtIN). Detergent-free wtIN was prepared as previously described (*25*). Mg^{2+} was used as divalent cation.

(C) Catalytic Core (CC). The fragment IN$^{50-212}$/F185K (CC) was overexpressed in *Escherichia coli* strain BL21 and purified as previously described (*26*). All enzyme concentrations are given on a subunit basis.

Integration Assays. (A) dmIN. The Reaction Buffer is 20 mM Hepes, 10 mM $MgCl_2$, 1 mM DTT, pH 7.5. For the strand transfer assay, dmIN (280 nM) was preincubated with the peptides at different IN:peptide molar ratios and the target plasmid DNA pSP65 (15 ng), for 30 min at 30 °C. A double-stranded preprocessed oligonucleotide, S1/S2 (0.5 ng), was then added to the mixture, and the reaction was further incubated for 40 min at 30 °C. Reaction products were separated on a 1.2% agarose gel in 0.5× TBE, pH 8, and visualized by autoradiography.

For the 3′ processing and autointegration reactions, a labeled double-stranded S3/S2 oligonucleotide was used. Preincubation of dmIN (280 nM) with peptides at different concentrations and incubation with the S3/S2 oligonucleotides (5 ng) were carried out at 37 °C in Reaction Buffer, as above. Samples were heated for 3 min at 95 °C, separated in denaturing (7 M urea) 18% polyacrylamide gels in 1× TBE, pH 8, and visualized by autoradiography.

(B) wtIN. Peptides and 50 nM wtIN were preincubated for 5 min at 4 °C in Reaction Buffer containing 20 mM $MgCl_2$. The S3/S2-labeled duplex (5 ng) was added, and the

3′ processing was started by placing the reaction mixture at 37 °C and allowed to proceed for 60 min.

(C) Disintegration Assays. Disintegration reaction was carried out using the dumbbell substrate DIN (*27*). The dmIN (280 nM) or the CC domain (300 nM) was preincubated with peptides at different enzyme:peptide molar ratios for 30 min at 37 °C. The DNA-labeled dumbbell substrate (30 nM) was added to the mixture, and this was incubated for another 60 min at 37 °C. Final products were heated for 3 min at 95 °C and subjected to electrophoresis in denaturing (7 M urea) 15% polyacrylamide gels in 1× TBE, pH 8, and visualized by autoradiography. Quantification of the integration products was made with a PhosphorImager Scanner (Molecular Dynamics).

Secondary Structure Predictions. These were carried out with the AGADIR and GOR algorithms. AGADIR (*28*) considers short-range interactions between residues at different pH values and temperatures, and predicts the helicity per residue for peptides lacking tertiary interactions in solution. GOR (*29*) that derives from analyses of protein crystal structures is more suitable for peptides in the protein environment.

IN 3D Structure. The crystallographic structure of the catalytic core (PDB code 2ITG) was visualized and plotted using the Insight II program (Molecular Simulations Inc., San Diego, CA) on a Silicon Graphic work-station O_2 R10000.

CD Spectroscopy. CD spectra were recorded on a Jobin-Yvon CD6 dichrograph. The dmIN version of the enzyme was used for the study of the interactions with the INH5 and INH1 peptides. Peptide concentrations were varied from 10 to 200 μM. Peptide spectra were obtained in the following: (i) H_2O and 1 mM sodium phosphate buffer, pH 7.5, containing 0.2 mM EDTA, as a function of temperature, pH, and salt (NaCl) concentration; (ii) aqueous solutions of TFE (trifluoroethanol) from 0 to 90% (v/v); and (iii) 20 mM Hepes, pH 7.5, 0.5 M NaCl, and 1% glycerol. The latter, termed SEC buffer, was also used for the study of the protein:peptide complexes in fluorescence and SEC experiments. Prior to the CD measurement, the samples were subjected to centrifugation at 10000*g* for 10 min in a microcentrifuge. UV absorbance at 280 nm was checked before and after centrifugation, such as to exclude a possible loss of material through formation of insoluble aggregates. The relations $P_\alpha = -[\Delta\epsilon_{222} \times 10]/N$ (where P_α is the percentage of α-helix, $\Delta\epsilon_{222}$ ($M^{-1}\cdot cm^{-1}$) is the circular dichroism at 222 nm, and N is the number of residues in the peptide) (Figures 3 and 4) or $P_\alpha = -[\Delta\epsilon_{222} \times 10]$ (where P_α is the percentage of α-helix and $\Delta\epsilon_{222}$ is the circular dichroism per residue at 222 nm) (Figure 7) were used to estimate the α helix content (*28*). The effects of the peptides on the protein conformation were estimated from the spectra of the complexes, obtained at different protein:peptide ratios, after subtracting the spectral contribution of unbound peptides.

Size Exclusion Chromatography of IN−Peptide Complexes. SEC experiments were performed using the Superdex 200HR 10/30 and Superdex 75HR 10/30 columns (Pharmacia) on a Beckman HPLC system. Flow rates were 0.5 mL/min (Superdex 200) or 0.4 mL/min (Superdex 75) with the mobile phase corresponding to the SEC buffer (see CD Spectroscopy). The enzyme, dmIN at 30 μM or the CC domain at 10 μM, and the peptides were mixed at different molar ratios and incubated on ice for 15 min prior to injection into the column. As above, samples were subjected to centrifugation at 10000*g* for 10 min prior to injection to exclude the formation of insoluble aggregates, and 70 μL of each sample was analyzed. Absorbance of the column eluate was monitored at both 280 and 222 nm. Fractions were analyzed by SDS−PAGE for the presence of IN. The column was calibrated using the gel filtration LMW calibration kit (Pharmacia) (13 700−67 000 Da) and a purified IgG (150 000 Da). The void volume was determined using blue dextran 2000. The log of the known molecular weights of standard proteins was plotted versus the peak position [partition coefficient (K_{av})], and linear regression was applied to calculate the apparent molecular weights of relevant peaks in the samples.

Fluorescence Spectroscopy. (A) Self-Association and Heteroassociation of INH5, Using a Fluorescent Peptide Derivative. Fluorescence emission intensities of the anthraniloyl-labeled peptide INH5 (excitation 314 nm, emission 412 nm) were obtained with a Jobin-Yvon Fluoromax II instrument, at 15 °C. The peptide was dissolved at 100 nM concentration in the SEC buffer, and aliquots of unlabeled INH5 or, respectively, unlabeled INH1 were added successively. The fluorescence intensities were plotted against the total concentration, C, of added peptides and fitted to sigmoid curves according to the equation: $F = F_0 + \Delta F C^h/(C_{0.5}{}^h + C^h)$, where F_0 is the initial fluorescence of the anthraniloyl-labeled peptide INH5, ΔF is the total amplitude of its variation, $C_{0.5}$ is the concentration corresponding to the midpoint of the titration, and h measures the cooperativity of the interaction. When the concentration of the titrating partner exceeds that of the labeled one, $C_{0.5}$ is equal to the dissociation constant, K_d.

(B) Interaction of IN and of the CC Domain with INH5. The intrinsic fluorescence of wtIN and of the CC domain (at 115 nM concentration) was measured at 15 °C, in semi-micro cuvettes containing 800 μL of Reaction Buffer, with excitation at 295 nm and emission at 337 nm, with 2 and 5 nm slit widths. Fluorescence quenching following interaction with INH5 was expressed as $1 - F/F^0$, where F^0 is the fluorescence in the absence of added peptide.

RESULTS

Inhibition of Integration Reaction by INH1 and INH5. The inhibitory effects of the synthetic peptides INH1 and INH5, deriving from the IN CC domain (segments 93−107 and 167−187, incorporating the α1 and α5 helices, respectively, Figure 1), were tested on either dmIN or wtIN integration and disintegration (strand transfer) assays. Most relevant results regarding INH5, which acted as a better inhibitor than INH1, are presented in Figure 2. In the heterologous integration assay, INH5 inhibited the strand transfer activity of dmIN in the presence of Mn^{2+} with an IC_{50} value of 0.5 μM (Figure 2A), while an IC_{50} of only 120 μM was found for INH1 (data not shown). Figure 2B shows that INH5 inhibits the 3′ processing activity of dmIN in the presence of Mn^{2+} with an IC_{50} value of 11 μM and the strand transfer reaction with an IC_{50} of 4.7 μM. INH1 exhibits inhibitory properties at higher concentrations (IC_{50} = 250 μM for 3′ processing and 150 μM for strand transfer) (data not shown).

The inhibitory activity of INH5 was also tested on wtIN at a lower concentration (50 nM), in the presence of Mg^{2+}

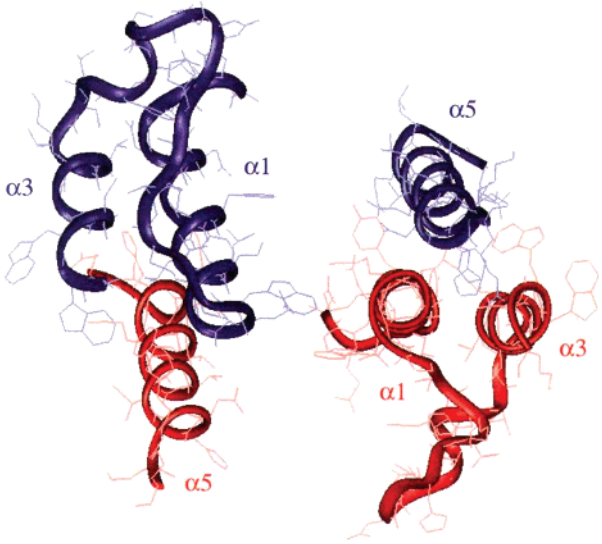

FIGURE 1: Structure of the dimerization domain of the HIV-1 IN catalytic core, as provided by the X-ray crystallography data of Bujacz et al. (*15*). Two monomers are shown, colored in red and blue. The important α1 and α5 helices, leading to the inhibitor peptides INH1 and INH5, respectively, are indicated together with the α3 helix.

as divalent cation. One found an IC_{50} value of about 85 nM for the inhibition of the 3′ processing step and of 60 nM for the strand transfer activity (Figure 2C).

It has been repeatedly shown that the CC domain of IN is able on its own to catalyze the disintegration reaction. INH5 inhibited the disintegration mediated by the enzyme (dmIN) and by the CC domain with IC_{50} values of 1.2 and 50 μM, respectively, while with INH1 the IC_{50} values were 250 and 475 μM, respectively (data not shown).

Structure Predictions on INH1 and INH5. The specific pairing of INH1 with α5 and of INH5 with α1 would require the peptides to be under helical conformations similar to those exhibited by their parent segments in the crystal structure (Figure 1). Only under such conditions can the correct adjustment of the interacting groups be achieved. According to AGADIR predictions (*28*), INH1 and INH5 have a low degree of helix secondary structure in aqueous solution (15−20% and 5−10%, respectively, at pH 7). In contrast, the GOR analysis (*29*) predicted a much higher helical content (70−75% for INH1 and 65−70% for INH5), consistent with the helical conformations adopted by the corresponding segments in the crystal structure. As the helical structures predicted by AGADIR concern peptide fragments and those predicted by GOR concern peptide segments within proteins, the difference between the two predictions outlines the strong impact of the protein context on the stability of the α1 and α5 helices. Actually, examination of the CC crystal structures (*14*−*17*) reveals a tight helix packing, especially at the dimer interface involving the α1 and α5 helices (Figure 1).

Experimental Secondary Structures of INH1 and INH5. CD spectra of INH1 and INH5 at 60 μM concentration in water at pH 3 (unmodified pH after peptide synthesis) and in aqueous solutions of TFE are presented in Figure 3. The hydrophobic organic solvent TFE has been extensively used to study the structure of short natural peptides (*29*, *30*). It is mostly known to stabilize the α helix secondary structure through the strengthening of intramolecular hydrogen bonds

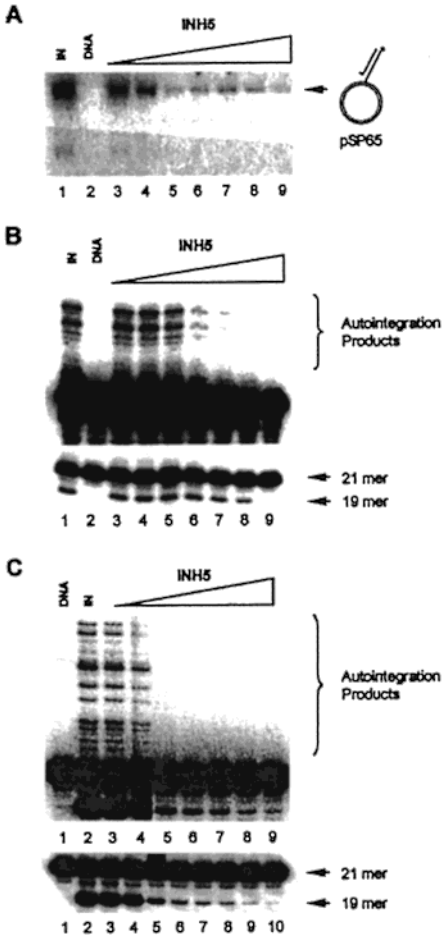

FIGURE 2: Effects of INH5 on integration and disintegration activities. (A) Heterointegration: lane 1, dmIN incubated with DNA; lane 2, DNA alone; lanes 3−9, dmIN incubated with INH5 at 0.5, 1, 4, 6, 9, 12, and 20 μM, respectively. (B) 3′ processing and autointegration: lane 1, dmIN incubated with DNA; lane 2, DNA alone; lanes 3−9, dmIN incubated with 0.5, 1, 4, 6, 9, 12, and 20 μM, respectively. (C) Lane 1, DNA alone; lane 2, wtIN incubated with DNA; lanes 3−10, wtIN incubated with INH at 0.03, 0.1, 0.3, 0.6, 1, 3, 6, and 10 μM, respectively, for 3′ processing and at 0.03, 0.1, 0.6, 1, 3, 6, and 10 μM, respectively, for autointegration.

(*12*, *31*−*34*). Spectra of INH1 and INH5 in water are typical of peptide structures largely unordered, with strong and weak minima around 200 and 222 nm, respectively. Addition of TFE promotes helix formation in both INH1 and INH5, although the maximum of helix content does not exceed 20%. The two peptides do not show the same susceptibility to TFE, as the plateau occurs at only 20−30% TFE for INH5 and at 60% TFE for INH1 (titration curves in the insets to Figure 3). This suggests a different balance of stabilizing and destabilizing effects of the side chains in INH1 and INH5. The helix content of the peptides, although largely augmented by TFE, does not reach that expected from examination of the crystal structure or that predicted by the GOR algorithm. A plausible explanation for this difference could be the strong contribution of the packing to the helix stabilization, already suggested by examination of the CC domain crystal structure (Figure 1).

The contribution of side-chain−side-chain interactions to helix stability is reflected by the change in CD spectra of peptides recorded as a function of pH, salt concentration, and temperature (not shown). These factors exert to different

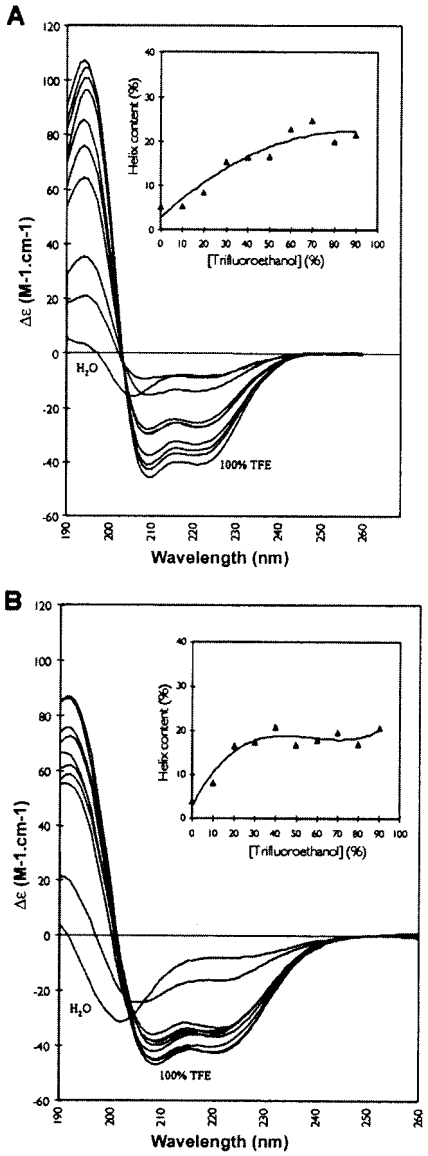

FIGURE 3: Trifluoroethanol (TFE) effect on circular dichroism (CD) spectra of peptides INH1 (A) and INH5 (B), recorded at 25 °C in water and in water/TFE mixtures. Percentage TFE within H_2O was varied from 0 to 90% by 10% increments. The peptide concentration was maintained at 60 μM. Helical contents were determined by direct reading of ellipticities at 222 nm (see Experimental Procedures). Curves given in insets represent the variation of the helical contents in INH1 (A) and INH5 (B) as a function of the percentage of TFE.

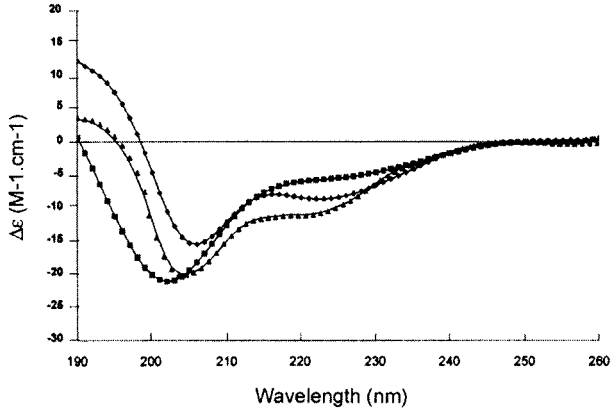

FIGURE 4: Interaction of INH1 with INH5. CD spectra of INH1 (triangles) and INH5 (squares) alone at 60 μM and of an equimolar mixture of the two peptides (diamonds) were recorded at 25 °C in H_2O at pH 3.5.

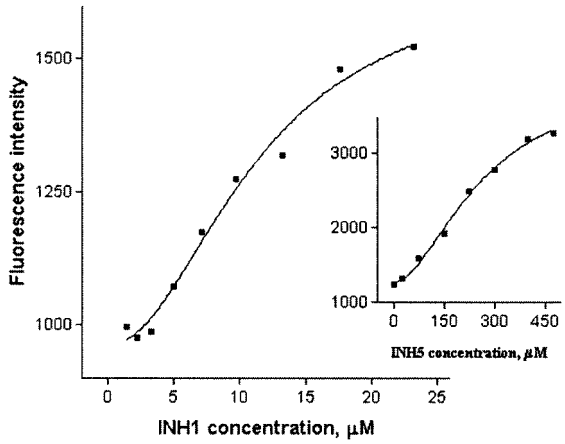

FIGURE 5: Fluorescence enhancement of anthraniloyl-INH5, at 100 nM in SEC buffer, as a result of its interaction with INH1 (heterointeraction, $C_{0.5} = 11.4 \pm 2.4$ μM, $h = 2.0 \pm 0.6$) and with unlabeled INH5 (autoassociation, $C_{0.5} = 266 \pm 55$ μM, $h = 1.78 \pm 0.35$, inset).

extents an influence on peptide secondary structures. For instance, at 5 °C in SEC buffer, the CD spectra of INH1 and INH5 present a higher degree of helix stabilization compared to that obtained in pure water (this will be seen in Figure 9).

Associative Properties of INH1 and INH5. The CD spectra obtained as a function of peptide concentration in both water and TFE do not reflect any significant change and are not compatible with the autoassociation of either INH1 or INH5 (data not shown). In contrast, the CD spectrum of INH1 and INH5 mixed in equimolecular amounts is not equivalent to the sum of the individual spectra and is therefore compatible with the pairing of the peptides (Figure 4). The spectral changes include a shift of the largest negative minimum to about 207 nm and the increase of the positive band situated around 190 nm. These are signs of helix stabilization at the detriment of unordered structures, likely by mutual interactions of INH1 and INH5. Actually, the higher propensity of INH1 and INH5 for heteroassociation rather than autoassociation is consistent with the α1:α5′ helix pairing observed at the dimer interface (Figure 1).

The autoassociation of INH5 and the interaction of INH5 with INH1 have further been examined by fluorescence spectroscopy using anthraniloyl-labeled INH5. Upon binding of INH1 to labeled INH5, the fluorescence intensity of the anthraniloyl moiety is enhanced by 73% (Figure 5). The shape of the curve is sigmoidal ($h = 2.0 \pm 0.6$), with a midpoint of titration, $C_{0.5}$, measuring the affinity of the two peptides, at 11.4 ± 2.4 μM. The sigmoidal shape of the curve may be viewed as an indication of the fact that the hetero-interaction requires a nucleation step, as proved by the structuration of the peptides upon mixing INH5 and INH1 in CD experiments (Figure 4). The two partners need to meet in the right orientation and undergo a process of self-folding and adjustment prior to the "zipperring-up" of the two molecules together. The inset to Figure 5 shows that the basic features are preserved in the homo-interaction, when mixing labeled INH5 with its unlabeled counterpart ($h = 1.78 \pm 0.35$). The fluorescence enhancement is as large as 220%,

reflecting the proximity of the fluorophore to the interacting peptide (in the preceding case, the sizes of the interacting peptides were different: 17 residues for INH1 vs 22 residues for anthraniloyl-INH5). The major difference consists of the low affinity of the homo-interaction: in this case, $C_{0.5}$ equals 266 ± 55 μM. Thus, in terms of dissociation constants, the hetero-interaction is 23 times stronger than the interaction of the INH5 peptide with itself.

Interactions of INH1 and INH5 with IN and with the CC Domain. Size exclusion chromatography (SEC) was used to examine the effect of INH1 and INH5 on the oligomeric state distribution of dmIN and CC (Figures 6 and 7). No pellet was observed in the tubes after centrifugation, and the absorbance at 280 nm measured before and after centrifugation remained unchanged for both the unbound and bound protein, indicating that insoluble aggregates did not form. The elution profile for IN alone presented four major peaks with retention times of 15.2, 23.7, 28.9, and 34.5 min, consistent with an equilibrium of large molecular weight oligomers, tetramers, dimers, and monomers (Figure 6A). The apparent molecular mass of the tetramer was 133 kDa, 56 kDa for the dimer, and 28 kDa for the monomer. These experimental values compared favorably with calculated molecular masses of 128.8 kDa for the tetramer, 64.4 kDa for the dimer, and 32.2 kDa for the monomer. The values of the retention times of dimers and tetramers are identical to those reported for the same soluble dmIN under similar experimental conditions (*24*). When IN was incubated in the presence of increasing amounts of INH5 (Figure 6B,C) or INH1 (Figure 6D,E) at the inhibitory molar ratios observed in in vitro assays, a progressive disappearance of the oligomer, tetramer, and dimer peaks was observed at the benefit of the monomer peak. The effects were weaker with INH1 compared to INH5. At a 1:5 ratio of protein:INH5, the equilibrium was completely shifted toward the monomer. A retention time value of 39.3 min was found for the liganded monomer at a ratio of 1:5 instead of 34.5 min for the unbound protein. A similar retardation effect has been observed by Asante-Appiah and Skalka (*35*) when adding Mn^{2+} to the same dmIN. The authors have imputed the retarded retention time to a conformational change of the enzyme caused by Mn^{2+}.

In an SEC experiment performed with the CC domain, INH5 and INH1 were capable of inducing dissociation of CC oligomer into CC monomers at the same molar ratios as used in biological assays (Figure 7A−C), thus confirming the key role of the CC domain in maintaining the oligomeric structure of the entire enzyme.

Quenching of the intrinsic fluorescence of IN and of its CC domain, presumably as a result of their dissociation into subunits, made it possible to quantify the interactions with INH5. The results are shown in Figure 8. With protein at 115 nM, the midpoints of the titrations are at $C_{0.5} = 44 \pm 7$ and 168 ± 40 nM subunit concentration of CC and IN, respectively (Figure 8A). On the other hand, the affinity of INH5 for IN diluted to 10 nM was higher (data not shown). The results show that INH5 recognizes both the CC and the whole IN molecules, although it has more difficulty in getting bound to the latter. In any case, it follows that the binding site is within the enzyme CC domain. In line with this, the percent quenching with CC is greater than that obtained with the whole enzyme, suggesting that the bulk of the structure

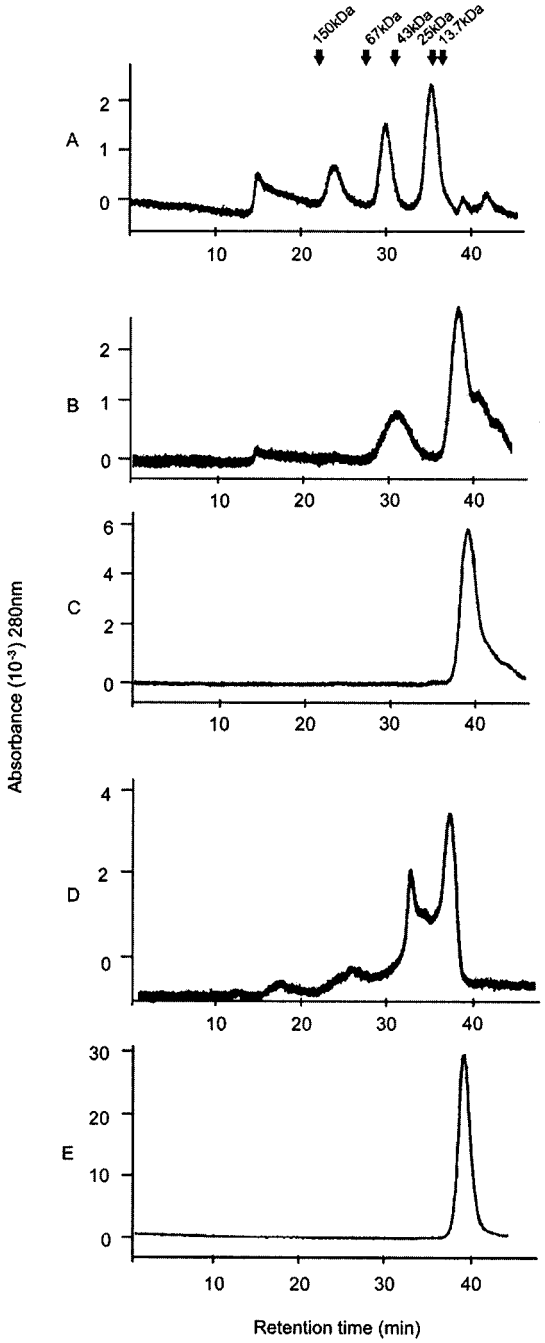

FIGURE 6: Effect of INH1 and INH5 on HIV-1 dmIN oligomerization in SEC buffer. (A) Size exclusion chromatography of dmIN (30 μM) alone. The peak elution times of ribonuclease A (13.7 kDa), chymotrypsinogen (25 kDa), ovalbumin (43 kDa), bovine serum albumin (67 kDa), and purified IgG (150 kDa) are indicated. (B) dmIN incubated with INH5 at a 1:1 molar ratio. (C) dmIN incubated with INH5 at a 1:5 molar ratio. (D) dmIN in the presence of INH1 at a 1:5 molar ratio. (E) dmIN incubated with INH1 at a 1:10 molar ratio. All the monomer peaks obtained in the presence of INH1 and INH5 exhibit a delayed elution time probably due to a conformational change of dmIN in the presence of these peptides (see text).

alteration induced by dissociation into subunits takes place within the former.

Conformational Changes of IN Induced by Peptides. The question of the possible change of enzyme secondary structure induced by peptide addition was addressed using CD spectroscopy. CD experiments (Figure 9) showed that, in the SEC buffer, dmIN displays nearly 37% of helix

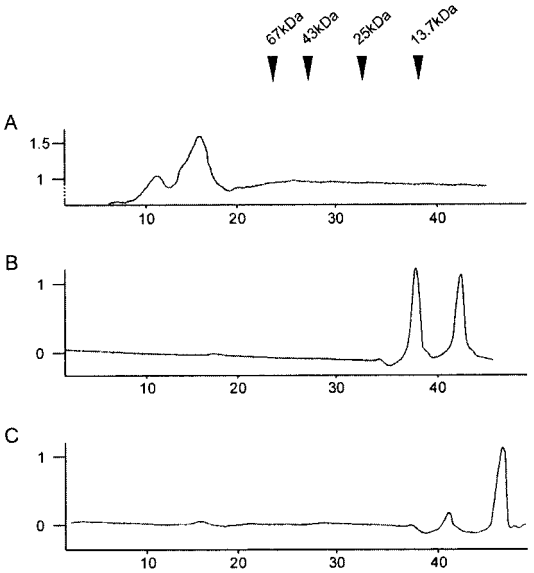

FIGURE 7: Effect of INH1 and INH5 on HIV-1 CC domain oligomerization in SEC buffer. (A) SEC of CC (10 μM) alone. (B) CC incubated with INH5 at a 1:40 molar ratio. (C) CC incubated with INH1 at a 1:40 molar ratio. The molecular mass markers are the same as in Figure 6.

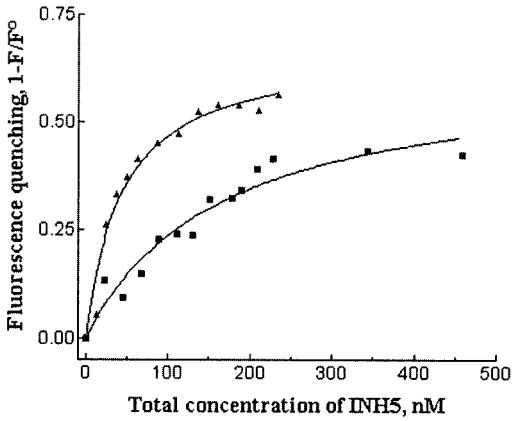

FIGURE 8: Percentage of quenching of the intrinsic fluorescence of CC (triangles) and of wtIN (squares), each at 115 nM subunit concentration, upon interaction with INH5 in Reaction Buffer. The wtIN contains six Trp and CC three Trp. Semi-saturation is achieved at $C_{0.5} = 44 \pm 7$ nM and 168 ± 40 nM, respectively.

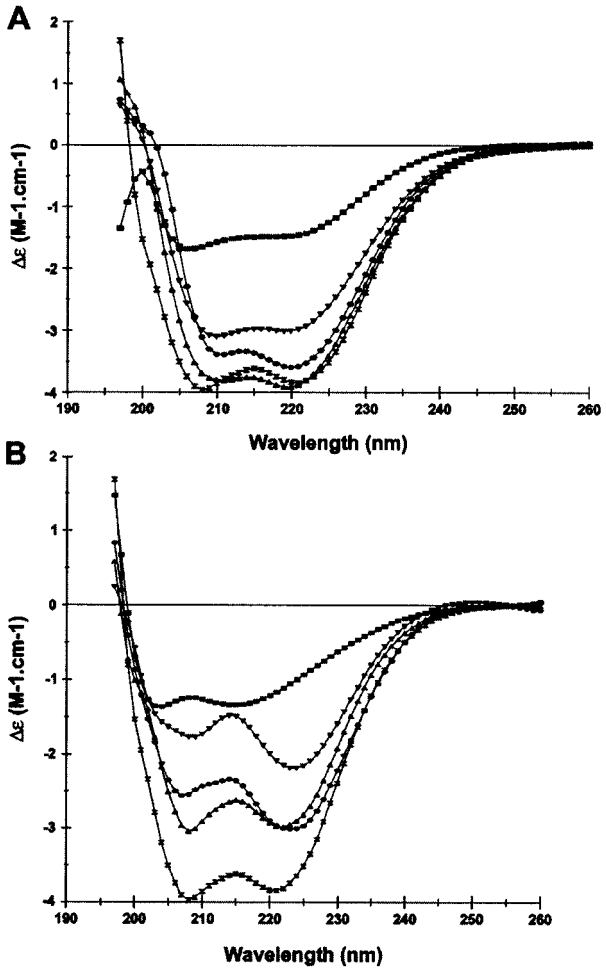

FIGURE 9: Interaction of INH1 and INH5 with dmIN. CD spectra were recorded at 5 °C in SEC buffer. Conformational effects of the peptides on the protein were estimated from the CD spectra of the complexes recorded at different protein:peptide ratios and subtracting the peptide initial contribution. (A) CD spectra of INH1 alone at 200 μM (squares) and of dmIN alone at 20 μM (inverted triangles). Complexes of dmIN (20 μM) with INH1 at a 1:2 ratio (triangles), 1:4 ratio (circles), and 1:10 ratio (double triangles). (B) CD spectra of INH5 alone at 80 μM (circles) and of dmIN alone at 20 μM (triangles). Complexes of dmIN (20 μM) with INH5 at a 1:1 ratio (double triangles), 1:2 ratio (inverted triangles), and 1:4 ratio (squares).

content. This value is identical to that found with structure-predicting algorithms (*36*). It is also similar to the one estimated from examination of the crystal (CC domain and CC plus C-terminal domains) and NMR (N-terminal and C-terminal domains) structural data (*14*−*21*). Addition of INH5 or INH1 to solutions of dmIN gave rise to significant CD spectral changes compatible with a significant loss of helix secondary structure in the protein. As expected from the SEC and the biological assay results, the changes produced by INH5 (Figure 9B) are much larger compared to those produced by INH1 (Figure 9A), which is also compatible with the higher affinity of INH5 for IN compared to INH1.

DISCUSSION

For several years now our laboratory has been interested in peptide-based inhibitors against the IN enzyme of HIV-1 (*12*, *37*−*39*). We were somehow encouraged by the reported peptide-based inhibitors of HIV protease and reverse transcriptase targeting the oligomerization (*40*−*42*). Here, we postulated that peptides deriving from the dimerization interface of the CC domain would function as specific inhibitors of the whole enzyme in preventing its self-association. Two peptides, INH1 and INH5, were synthesized. These incorporate the segments leading to the α1 and α5 helices, respectively. The α1 helix of one monomer interacts with the α5 helix of the other and vice versa (Figure 1). In in vitro integration assays, INH5 behaves as one of the strongest peptide inhibitors of the IN activity reported so far (*9*, *22*). This is true with either the double mutant dmIN in the presence of Mn^{2+} or the wild-type wtIN with Mg^{2+} as divalent cation. The IC_{50} is lower than 100 nM for the latter at 50 nM enzyme concentration. In comparison, the hexapeptide HisCysLysPheTrpTrp displays an IC_{50} of barely 3 μM (*9*, *22*).

The results of disintegration assays with the CC domain in the presence of Mn^{2+} demonstrated that the INH5 target is contained within the CC domain. Such experiments do

not solve the problems of the exact target in CC and of the mechanism of inhibition. These were addressed by CD and fluorescence spectroscopies and SEC experiments. CD is commonly used to assess secondary structures and conformational changes of proteins (*43*) while fluorescence is convenient for measuring the affinity of ligands for proteins (*44*) and SEC is increasingly used for the analysis of multimerization properties of proteins, including IN (*24, 26, 35, 45, 46*).

The way in which INH1 and INH5 alter the multimerization of IN was revealed by SEC. The association−dissociation equilibrium of IN may be viewed as an interlocked set of discrete types of macromolecular dynamic rearrangements in a subunit ensemble, IN_x, and its stepwise-dissociation species:

$$IN_x \Leftrightarrow IN_{x-1} + IN \Leftrightarrow IN_{x-2} + 2IN \Leftrightarrow ... \Leftrightarrow xIN$$

Incubation of INH5 with dmIN at different molar ratios severely altered the equilibrium. At a protein:peptide ratio of 1:1, tetramers and higher order oligomers were already totally absent from the chromatogram. At a ratio of 1:5, the dimers were also suppressed, leaving the monomers as the only existing species. As the equilibrium is shifted toward the monomer, it could be concluded that the ligand combines more strongly with the monomer than with the oligomers. All of this indicates that functional oligomers are dissociated by INH5 and INH1 with as a major consequence the loss of IN activity.

Dissociation of multimers does not seem to be the only effect exerted by the two peptides. The retarded mobility exhibited by the monomer in the presence of INH1 or INH5 in SEC experiments suggested that the individual monomer assumed an altered conformation. This was confirmed by the CD spectra of dmIN incubated with INH1 and INH5. Thus, the destabilization of the enzyme secondary structure, and particularly that of α helices, parallels the oligomer dissociation. Liganded monomers do not have the same secondary/tertiary structure and stability they have in native dimers or oligomers. A loss of α helix content accompanying dissociation seems quite reasonable for IN considering that secondary structure stabilization, protein folding, and oligomerization evolve together and can be concerted processes. Actually, most biological homodimers are only observed in the multimeric states, and it is generally impossible to dissociate them without denaturing the individual monomer structure. The dimer interface of the IN CC domain is stabilized through numerous interhelical contacts involving the α1 and α5 helices, which further participate with the native structure of each subunit through stabilizing interactions with other helices of the protein (Figure 1). In fact, the interface is composed of closely packed atoms similar to those found deeper in the CC domain. The biologically relevant amphipathic α4 helix is connected through a 10 residue loop to the α5 helix and participates in the protein packing by interacting with the α5 helix. The α4 helix spans four helical heptads, prone to form coiled-coil structures with helices from other subunits (*12, 37*−*39*). As a matter of fact, it is possible that dimers, held together by α1:α5 interactions, further associate via α4:α4 coiled-coil interactions, to create higher order oligomers (*39*). Thus, due to the large array of interdependent stabilizing interactions within and between the subunits, the IN molecule may undergo a profound secondary structure change upon dissociation of its multimers, explaining the retarded retention time of the monomers in SEC, the spectral changes observed in CD, and the quenching of the intrinsic fluorescence.

Nevertheless, the ability of our peptides to so deeply change the conformation of the enzyme was a rather unexpected finding. What is clear is the high affinity of INH5 for its cognate dmIN and the consecutive dissociative and inhibitory effects. Thus, the next point was logically the identification of the peptide targets and the initial events responsible for the cascade of the observed physicochemical and biological effects. That the α1 and α5 helices of the CC domain constitute possible targets for the peptide inhibitors ought to be reflected by the ability of INH1 and INH5 to combine together. Despite their weaker secondary structure, as compared to that of their parent α1 and α5 helices at the dimer interface, the INH1 and INH5 peptides maintained an ability to interact with each other. The observed CD changes proved that the INH1 and INH5 peptides preferred heteroassociation to autoassociation. The fluorescence experiments confirmed that the interaction of INH1 with INH5 is much stronger (23 times larger in terms of dissociation constants) than the interaction of INH5 with itself. Such features were consistent with pairings of INH1 with the α5 helix and of INH5 with the α1 helix of the CC domain. The affinity of INH5 for the enzyme or for the CC domain is much higher than for INH1, which is explained by the fact that the interaction of INH5 with its target within the enzyme context finds the latter in helical state, and less free energy has to be spent before achieving the adjustment of interacting groups. On the other hand, the better affinity of INH5 for IN at 10 nM compared with IN at 115 nM could be explained by the fact that the dilution dissociates the enzyme (*25*). With the concentrated enzyme, additional free energy is necessarily spent for the dissociation of the enzyme oligomers. The two pieces of data are compatible with the supposed dissociative mechanism of enzyme inhibition by INH5.

Finally, our results highlight the good correlation between the biological and structural effects produced by the peptides INH1 and INH5 on IN: the more efficient the oligomer dissociation and the secondary structure alteration, the stronger the enzyme deactivation.

INH5 could be the model molecule for conceiving peptidomimetics presenting the same function, resisting to protease degradation and transduced across the cell membranes. As INH5 disrupts aggregates and higher order oligomers of IN, it could be used in small amounts for the solubilization of the protein. Attempts of crystallizing the full-length wild-type IN are confronted to its low solubility, and cocrystallization of INH5 with IN could be providential.

ACKNOWLEDGMENT

We thank O. Mauffret for comments on the manuscript and J. P. Levillain for skilled assistance in peptide synthesis.

REFERENCES

1. Goff, S. P. (1992) *Annu. Rev. Genet. 26*, 527−554.
2. Turner, B. G., and Summers, M. F. (1999) *J. Mol. Biol. 285*, 1−32.

3. Brown, P. O. (1997) in *Retroviruses* (Coffin, J. M., Hughes, S., and Varmus, H. E., Eds.) Vol. 1, pp 161−230, Cold Spring Harbor Laboratory, Cold Spring Harbor, NY.
4. Esposito, D., and Craigie, R. (1999) *Adv. Virus Res. 52*, 319−333.
5. Wlodawer, A. (1999) *Adv. Virus Res. 52*, 335−350.
6. Asante-Appiah, E., and Skalka, A.-M. (1999) *Adv. Virus Res. 52*, 351−365.
7. Katzman, M., and Katz, R. (1999) *Adv. Virus Res. 52*, 371−388.
8. Engelman, A. (1999) *Adv. Virus Res. 52*, 411−423.
9. Pommier, Y., and Nouri, N. (1999) *Adv. Virus Res. 52*, 427−448.
10. Goldgur, Y., Craigie, R., Cohen, G. H., Fujiwara, T., Yoshinaga, T., Fujishita, T., Sugimoto, H., Endo, T., Murai, H., and Davies, D. R. (1999) *Proc. Natl. Acad. Sci. U.S.A. 96*, 13040−13043.
11. Hazuda, D. J., Felock, P., Witmer, M., Wolfe, A., Stillmock, K., Grobler, J. A., Espeseth, A., Gabryelski, L., Schleif, W., Blan, C., and Miller, M. D. (2000) *Science 287*, 646−650.
12. Maroun, R. G., Krebs, D., El Antri, S., Deroussent, A., Lescot, E., Troalen, F., Porumb, H., Goldberg, M. E., and Fermandjian, S. (1999) *J. Biol. Chem. 274*, 34174−34185.
13. Chow, S. A., Vincent, K. A., Ellison, V., and Brown, P. O. (1992) *Science 255*, 723−726.
14. Dyda, F., Hickman, A. B., Jenkins, T. M., Engelman, A., Craigie, R., and Davies, D. R. (1994) *Science 266*, 1981−1986.
15. Bujacz, G., Alexandratos, J., Qing, Z. L., Clement-Mella, C., and Wlodawer, A. (1996) *FEBS Lett. 398*, 175−178.
16. Goldgur, Y., Dyda, F., Hickman, A. B., Jenkins, T. M., Craigie, R., and Davies, D. R. (1998) *Proc. Natl. Acad. Sci. U.S.A. 95*, 9150−9154.
17. Maignan, S., Guilloteau, J.-P., Zhou-Liu, Q., Clement-Mella, C., and Mikol, V. (1998) *J. Mol. Biol. 282*, 359−368.
18. Lodi, P. J., Ernst, J. A., Kuszewski, J., Hickman, A. B., Engelman, A., Craigie, R., Clore, G. M., and Gronenborn, A. M. (1995) *Biochemistry 34*, 9826−9833.
19. Eijkelenboom, A. P., Lutzke, R. A., Boelens, R., Plasterk, R. H., Kaptein, R., and Hard, K. (1995) *Nat. Struct. Biol. 2*, 807−810.
20. Cai, M. L., Zheng, R., Caffrey, M., Craigie, R., Clore, G. M., and Gronenborn, A. M. (1997) *Nat. Struct. Biol. 4*, 567−577.
21. Chen, J. C.-H., Krucinski, J., Miercke, L. J. W., Finer-Moore, J. S., Tang, A. H., Leavitt, A. D., and Stroud, R. (2000) *Proc. Natl. Acad. Sci. U.S.A. 97*, 8233−8238.
22. Puras Lutzke, R. A., Eppens, N. A., Weber, P. A., Houghten, R. A., and Plasterk, R. H. A. (1995) *Proc. Natl. Acad. Sci. U.S.A. 92*, 11456−11460.
23. Stennicke, H. R., Olesen, K., Sorensen, S. B., and Breddam, K. (1997) *Anal. Biochem. 248*, 141−148.
24. Jenkins, T., Engelman, A., Ghirlando, R., and Craigie, R. (1996) *J. Biol. Chem. 271*, 7712−7718.
25. Leh, H., Brodin, P., Bischerour, J., Deprez, E., Tauc, P., Brochon, J.-C., LeCam, E., Coulaud, D., Auclair, C., and Mouscadet, J.-F. (2000) *Biochemistry 39*, 9285−9294.
26. Jenkins, T. M., Hickman, A. B., Dyda, F., Ghirlando, R., Davies, D. R., and Craigie, R. (1995) *Proc. Natl. Acad. Sci. U.S.A. 92*, 6057−6061.
27. Chow, S. A., and Brown, P. O. (1994) *J. Virol. 68*, 3896−3907.
28. Muñoz, V., and Serrano, L. (1994) *Nat. Struct. Biol. 1*, 399−409.
29. Biou, V., Gibrat, J. F., Levin, J., Robsonand, B., and Garnier, J. (1988) *Protein Eng. 2*, 185−191.
30. Zhong, L., and Johnson, W. C. (1992) *Proc. Natl. Acad. Sci. U.S.A. 89*, 4462−4465.
31. Padmanabhan, S., Jimenez, M. A., Laurents, D. V., and Rico, M. (1998) *Biochemistry 37*, 17318−17330.
32. Luo, P., and Baldwin, R. L. (1997) *Biochemistry 36*, 8413−8421.
33. Jasanoff, A., and Fersht, A. R. (1994) *Biochemistry 33*, 2129−2135.
34. Cammers-Goodwin, A., Allen, T. J., Oslick, S. L., McClure, K. F., Lee, J. H., and Kemp, D. S. (1996) *J. Am. Chem. Soc. 118*, 3082−3090.
35. Asante-Appiah, E., and Skalka, A. M. (1997) *J. Biol. Chem. 272*, 16196−16205.
36. Lin, T. H., Quinn, T. P., Grandgenett, D., and Walsh, M. T. (1989) *Proteins: Struct., Funct., Genet. 5*, 156−165.
37. Sourgen, F., Maroun, R. G., Frère, V., Bouziane, M., Auclair, C., Troalen, F., and Fermandjian, S. (1996) *Eur. J. Biochem. 260*, 145−155.
38. Krebs, D., Maroun, R. G., Sourgen, F., Troalen, F., Davoust, D., and Fermandjian, S. (1998) *Eur. J. Biochem. 253*, 236−244.
39. Maroun, R. G., Krebs, D., Roshani, M., Porumb, H., Auclair, C., Troalen, F., and Fermandjian, S. (1999) *Eur. J. Biochem. 260*, 145−155.
40. Schramm, H. J., Boetzel, J., Buttner, J., Fritsche, E., Gohring, W., Jaeger, E., Konig, S., Thumfart, O., Wenger, T., Nagel, N. E., and Schramm, W. (1996) *Antiviral Res. 30*, 155−170.
41. McPhee, F., Good, A. C., Kuntz, I. D., and Craik, C. S. (1996) *Proc. Natl. Acad. Sci. U.S.A. 93*, 11477−11481.
42. Divita, G., Baillon, J. G., Rittinger, K., Chermann, J.-C., and Goody, R. S. (1995) *J. Biol. Chem. 270*, 28642−28646.
43. Venyaminov, S. Y., and Young, J. T. (1996) in *Circular Dichroism and the Conformational Analysis of Biomolecules* (Fasman, G. D., Ed.) pp 69−107, Plenum Press, New York and London.
44. Eftink, M. R. (1997) *Methods Enzymol. 278*, 221−257.
45. Andrake, M., and Skalka, A. M. (1995) *J. Biol. Chem. 270*, 29299−29306.
46. Taddeo, B., Carlini, F., Verani, P., and Engelman, A. (1996) *J. Virol.* 70, 8277−8284.
47. Schwarze, S. R., Hruska, K. A., and Dowdy, S. F. (2000) *Trends Cell Biol. 10*, 290−295.

BI011328N